Estuarine, Coastal and Shelf Science 309 (2024) 108976

Contents lists available at ScienceDirect

Estuarine, Coastal and Shelf Science

journal homepage: www.elsevier.com/locate/ecss

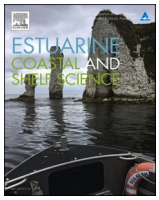

Mechanisms enabling the self-recruitment of passive larvae in the Great Barrier Reef

Eric Wolanski [a,*], Miguel De Le Court [b], Jonathan Lambrechts [b], Michael Kingfsord [a]

[a] College of Science and Engineering, James Cook University, Townsville, Queensland, 4811, Australia
[b] Institute of Mechanics, Materials and Civil Engineering, Université Catholique de Louvain, Avenue Georges Lemaître 4, 1348, Louvain-la-Neuve, Belgium

ARTICLE INFO

Keywords:
Flow separation
Headlands
Jets
Eddies
Tides
Trapping

ABSTRACT

This paper evaluates the conditions experienced by water-born passive larvae of broadcast spawning coral and crown-of-thorn starfish and how they self-recruit to their natal reefs in the Great Barrier Reef. The hypothesis that passive larvae are trapped for extended periods around specific areas of their natal reef (100s of metres) was found to be generally invalid. However, at some sites long-term trapping may occur when flow separation at headlands and in reef passages creates recirculating flows in embayments and behind concave-shaped reefs. Linear reefs do not trap passive larvae. This was demonstrated using satellite images and oceanographic modeling. The degree of self-recruitment at locations depended on the details of the incident flow speed, the shape of the headlands and the reef passages, the orientation of the reef compared to that of the tidal currents, the aspect ratio of the embayment, the curvature of the reef, and the time that the developing mushroom tidal jets takes to pass in front of the embayment. Self-recruitment of passive larvae depends on the spatial scale; at scales of 100s of metres, it is a rare process in the Great Barrier Reef. An exception was in a high-density reef matrix where the sticky water effect prevailed and self-recruitment was higher. Further, at scales of whole reefs (kilometres) and clusters of reefs (kms to 10s of kilometres) the likelihood of self-recruitment was higher. The probability of self-recruitment for reef fish larvae swimming directionally to their natal reefs following auditory and chemical cues is predicted to be much higher.

1. Introduction

Little is known about the degree of self-recruitment by the larvae of broadcast spawners that include corals and crown-of-thorns starfish in the Great Barrier Reef (GBR) In part, this is due to the difficulties of measuring larval abundance and dispersal in the field and predicting it using oceanographic models. The small-scale topography of reefs plays a large role in larval retention (Wolanski and Hamner, 1988). The eggs and larvae are initially located near reefs after spawning (Saint-Amand et al., 2023; Wolanski et al., 2024). These larvae of corals have limited mobility and they are at the mercy of the water currents (Pratchett et al., 2024). The dominant process that may enable self-recruitment was believed to be the formation of island wakes (phase eddies; Fig. 1) and topographically controlled fronts (Wolanski and Hamner, 1988), which retain larvae around a reef and thus offer multiple chances for larvae to settle. However fluid mechanics dictate and field data and remote sensing confirm (Hamner and Hauri, 1977, 1981; Wolanski et al., 2024) that these eddies do not simply flip back and forth around the reef as the tidal currents reverse. Instead, they are generally advected away from the reef when the tidal currents reverse direction with the tide (Wolanski et al., 2024). A net current exports the water and its larvae away from the natal reef and, in such cases, passive larvae will not necessarily self-recruit to their natal reefs (Wolanski and Kingsford, 2014). In the rare case of zero net current, the eddies may rotate around a reef and thus keep the larvae close to the reef, likely facilitating self-recruitment (Burgess et al., 2007). There is however an important exception to that rule, namely for reefs packed together in a high-density archipelago of islands and reefs in shallow water. That is the hydrodynamic process of 'sticky waters', which enables the self-recruitment of passive larvae (Wolanski and Spagnol, 2000; Andutta et al., 2012; Wolanski et al., 2024). This process enables the retention of water-born larvae within an archipelago. It does not necessarily imply that the larvae self-recruit to their natal reefs, instead the larvae recruit throughout the archipelago at scales of kms to 10s of km.

Not all larvae are passive, reef fish larvae being a case in point. Reef fish can self-recruit to their natal reefs in surprisingly large numbers

* Corresponding author.
E-mail address: eric.wolanski@jcu.edu.au (E. Wolanski).

https://doi.org/10.1016/j.ecss.2024.108976
Received 29 May 2024; Received in revised form 25 September 2024; Accepted 30 September 2024
Available online 1 October 2024

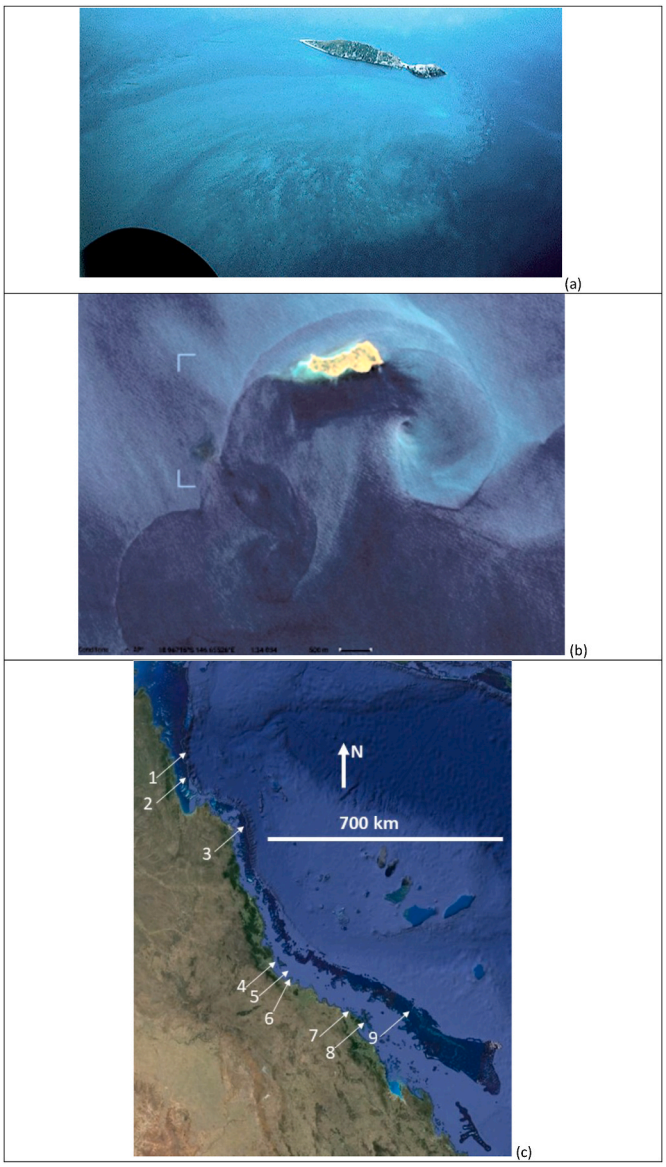

Fig. 1. (a) Aerial image of the wake at flood tide behind Rattray Island in the Whitsunday Islands group. The island is 1257 m from tip to tip along its long axis. (b) Sentinel-2 image at flood tide of the wake at flood tide behind Acheron Island. The island is 1144 m long from tip to tip along its long axis. (c) A GoogleEarth view of the northeast coast of Australia showing the location of the study sites in the Great Barrier Reef. 1: Bligh Reef; 2: Tijou Reef; 3: Ribbon Reef No. 10; 4: Palm Islands; 5: Acheron Island; 6: Magnetic Island; 7: Rattray Island; 8: Haselwood Island; 8: Cockatoo Reef.

(Jones et al., 2005; Karkarey and Theo, 2016). These larvae return to their natal reef to self-recruit by directional swimming at post-flexion following auditory and chemical cues, and possibly vertical movements to different depths with different current regimes (Paris et al., 2007; Gerlach et al., 2007; Leis et al., 2011; Wolanski and Kingsford, 2014; Bottesch et al., 2016; Kingsford et al., 2024; Ani et al., 2024). Their swimming behavior appears to rely on innate or learned compass directions, with no apparent map-based navigation (Spiecker et al., 2023). Fish larvae do not entirely control their fate because they are still at the mercy of the water currents, especially early in their development at pre-flexion (Schlaefer et al., 2018; Kingsford et al., 2024).

The patterns of transport and recruitment of coral fish larvae have been studied using advection-diffusion models whose results were verified by data on genetics (Bode et al., 2019). Such models can potentially predict the connectivity between reefs in the GBR of fish (Green et al., 2015) and crown-of-thorns starfish (Pratchett et al., 2024). There is a problem, however, with models of the GBR oceanography because most of them have a much coarser resolution (>500–1000 m, some are even coarser) than the spatial scales (typically 100–150 m) of the bathymetry that control flow separation and the advection-dispersion of passive, water-born larvae near reefs (Saint-Amand et al., 2023; Wolanski et al., 2024). Further some models have a coarse resolution that is greater than the separation of some reefs. As a result, many models don't provide reliable estimates of the self-recruitment potential and the connectivity within reefs of the GBR. With a focus on two specific groups, this leads to the question of what is the spatial scale that oceanographic models must have to realistically predict the degree of self-recruitment of coral and crown-of-thorns-starfish larvae. To answer that question, we relied on field data. For example, using 26 current meters, a detailed field study of the island wake dynamics was carried out at Rattray Island (Fig. 1a) where flow separation occurs (Wolanski et al., 1984, 2024). The data from that study were used to test numerical models of the island wake (Wolanski et al., 1996; Galloway et al., 1996; White and Wolanski, 2008). Models of the flow around islands and reefs in the GBR require small spatial resolution (typically less than 200 m) to reproduce the observations (Saint-Amand et al., 2023; Wolanski et al., 2024). Eddies behind islands and reefs are commonly observed in the GBR (Fig. 1a and b). Field studies, satellite images and numerical models of eddies behind such relatively linear reefs reveal that these eddies do not typically trap the larvae for more than a tidal cycle when the currents reverse with the tides.

Our objective is, through the analysis of satellite images at a number of sites and high-resolution oceanographic modeling, to identify the small-scale physical processes that enable the self-recruitment of passive larvae. Specifically, our aims are to: (1) identify the physical mechanisms that retain larvae for 10–14 days (2) examine if these mechanisms are reproduced among a range of topographies on the GBR (3) determine levels of self-recruitment at small (100s of m), medium (km) and large (tens of km) spatial scales. We show that (1) self-recruitment for passive larvae in these very dispersive environments is rare, and (2) for self-recruitment to occur, the reef or island must have a bay (an embayment or an oval-shaped bowl), with sharp headlands. The details of the bathymetry and of the small-scale hydrodynamics determine which part of a reef self-recruits. We also show that self-recruitment is higher as the scale of whole reefs.

2. Methods

We chose to study broadcast coral larvae and crown-of-thorns starfish larvae, as these are passively drifting larvae with a relatively short pelagic larval duration (Reichelt et al., 1990; Nozawa and Okubo, 2011). As detailed above, passive larvae are not trapped behind relatively short (1–2 km) and linear reefs and islands for more than a tidal cycle. Thus, we focused on convoluted islands and reefs, or very long, relatively straight reefs to identify possible self-recruitment sites in the GBR. The study sites are shown in Fig. 1c. Sentinel-2 and Landsat-8 images in the visible band of turbidity patterns around the selected reefs and islands were examined; these were enhanced for contrast using PaintShop Pro software. The SLIM oceanographic model of the GBR, first described by Lambrechts et al. (2008), was used to study the water currents and the dispersion patterns around these selected reefs and islands. The model uses a non-structured grid with a suitably small mesh size around reefs, it encompasses the whole GBR in order to use the correct forcing along the oceanic open boundary, and it enables the user to zoom in with a very small model mesh size on selected islands and reefs. The SLIM model has been verified against current meter data from moorings (e.g., Andutta et al., 2011, 2013; Wolanski et al., 2013, 2017; Wolanski and Lambrechts, 2020; Schlaefer et al., 2018 and 2020). The model was then used to estimate the potential for self-recruitment of passive water-born virtual larvae at the study sites. Following Okubo (1971), the sub-grid

scale horizontal diffusion coefficient was taken to be 0.1 m^2 s^{-1} for the small mesh size (typically ~ 150 m) of the model.

3. Results

i. Orpheus Island

Orpheus Island (Fig. S1a) in the Palm Islands group is 11 km long in its long axis, which is oriented alongshelf. It has a smoothly undulating east coast and a more rugged west coast with a bay, Pioneer Bay, between two headlands. The self-recruitment potential was calculated by counting the number of virtual larvae remaining in the small box (Fig. S1b) for small-scale self-recruitment and in the large box (Fig. S1b) for reef-scale self-recruitment. The waters around the island are quite shallow (<10 m within 200 m of the coast, see the bathymetry in Fig. S1c).

Sentinel-2 images revealed the common occurrence of topographically controlled currents around Orpheus Island, such as tidal jets in the passages between Orpheus Island and nearby islands (Fig. 2a), and mushroom tidal jets past headlands (Fig. 2b). Mushroom jets were unsteady jets formed when developing tidal currents flow past a headland (Wolanski et al., 2024). The landward eddy at the leading edge of the jets intruded in the embayment and flushed waters seaward. The outflow from a bay and coastal water also formed a mushroom jet (Fig. 2c).

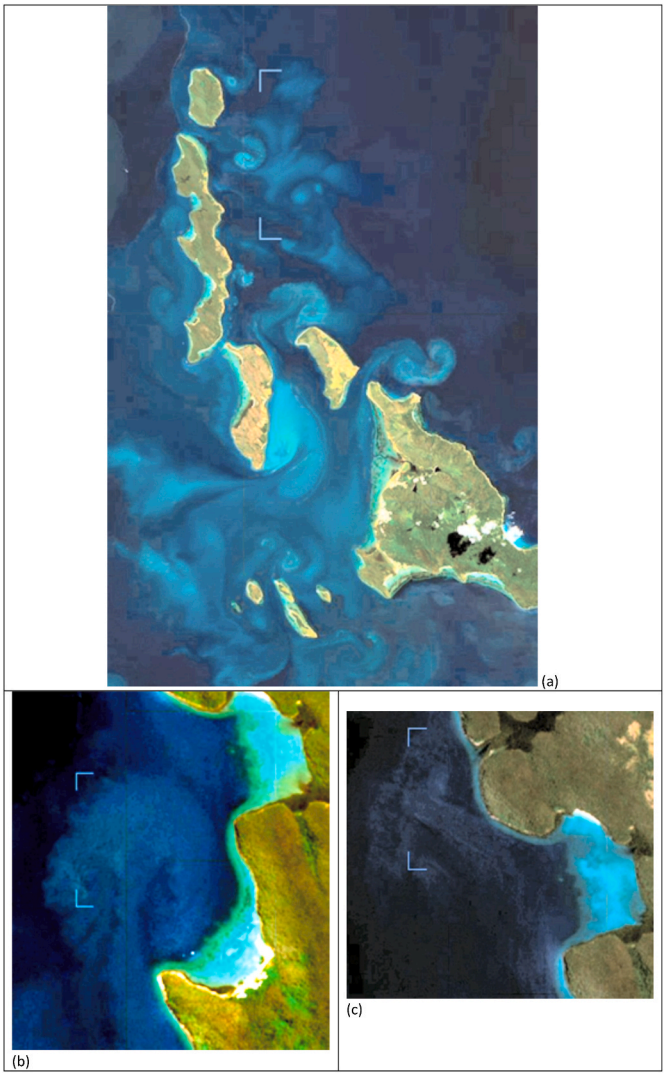

Fig. 2. Typical Sentinel-2 images of (a) mushroom jets, eddies and flow separation around Orpheus Island and surrounding islands during calm weather on ebb tide, (b) a mushroom jet in front of the southern region of Pioneer Bay, and (c) a mushroom jet exiting the northern end of Pioneer Bay. (b) and (c) are from different stages of the ebb tide, both in calm weather. The white brackets identify the mushroom tidal jets.

The SLIM oceanographic model had a very small mesh size around Orpheus Island (Fig. S1b). The file Animation S1 shows an animation of the tidal currents at 0.5 h interval for one tidal cycle. The scale shown in the first frame shows the speed in m/s. The red (see in the web version) areas are the shallows (depth <3 m). The model visually reproduced realistically the small-oceanographic features revealed by the satellite images, including eddies, jets, and shear layers both in front of shallows bays and downstream of headlands.

The file Animation S2 shows over 144 h and at 3 h intervals the predicted larval plume following a once-off instantaneous spawning of 30,000 virtual larvae in Pioneer Bay, which simulated mass spawning. The model revealed that water-born particles were trapped only in the northern side of Pioneer Bay, which is thus the only self-recruitment site at small scale. The degree of self-recruitment at small-scale after 8 days was about 0.25% (Fig. 3), which is half the number of larvae remaining around the whole island in the large box shown in Fig. S1b. The larvae remaining around the island, but outside Pioneer Bay, were too far from the fringing coral to recruit by simply settling down, although some larvae may still settle here and there because events of intense sub-grid scale topographically induced turbulence may bring some larvae to the fringing reefs.

ii Haselwood Island

Haselwood Island is a 6.2 km long and highly indented island in the Whitsundays Islands Group (Fig. S2a). The peak tidal currents are strong in that area following McGowan et al. (2023) whose SLIM model we used. Sentinel-2 images revealed the common occurrence of separation streamlines, eddies, mushroom jets and tidal jets (Fig. 4). The model mesh size around the island was very small (Fig. S2b). The predictions of the currents at 1 h interval for a tidal cycle in calm weather are shown in the file Animation S3; the colour bar shows the speed in m/s. The

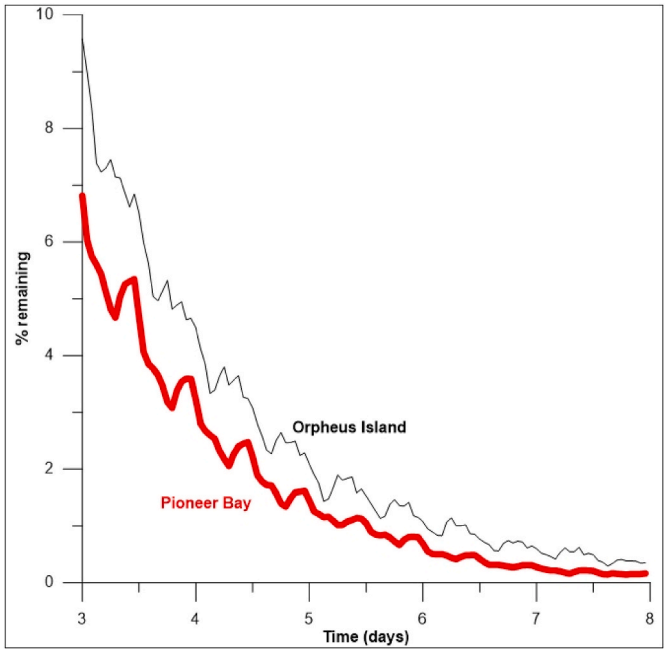

Fig. 3. Time-series plot of the predicted number of virtual larvae remaining in Pioneer Bay (the small box in Fig. S1b) and around Orpheus Island (the large box in Fig. S1b) in calm weather.

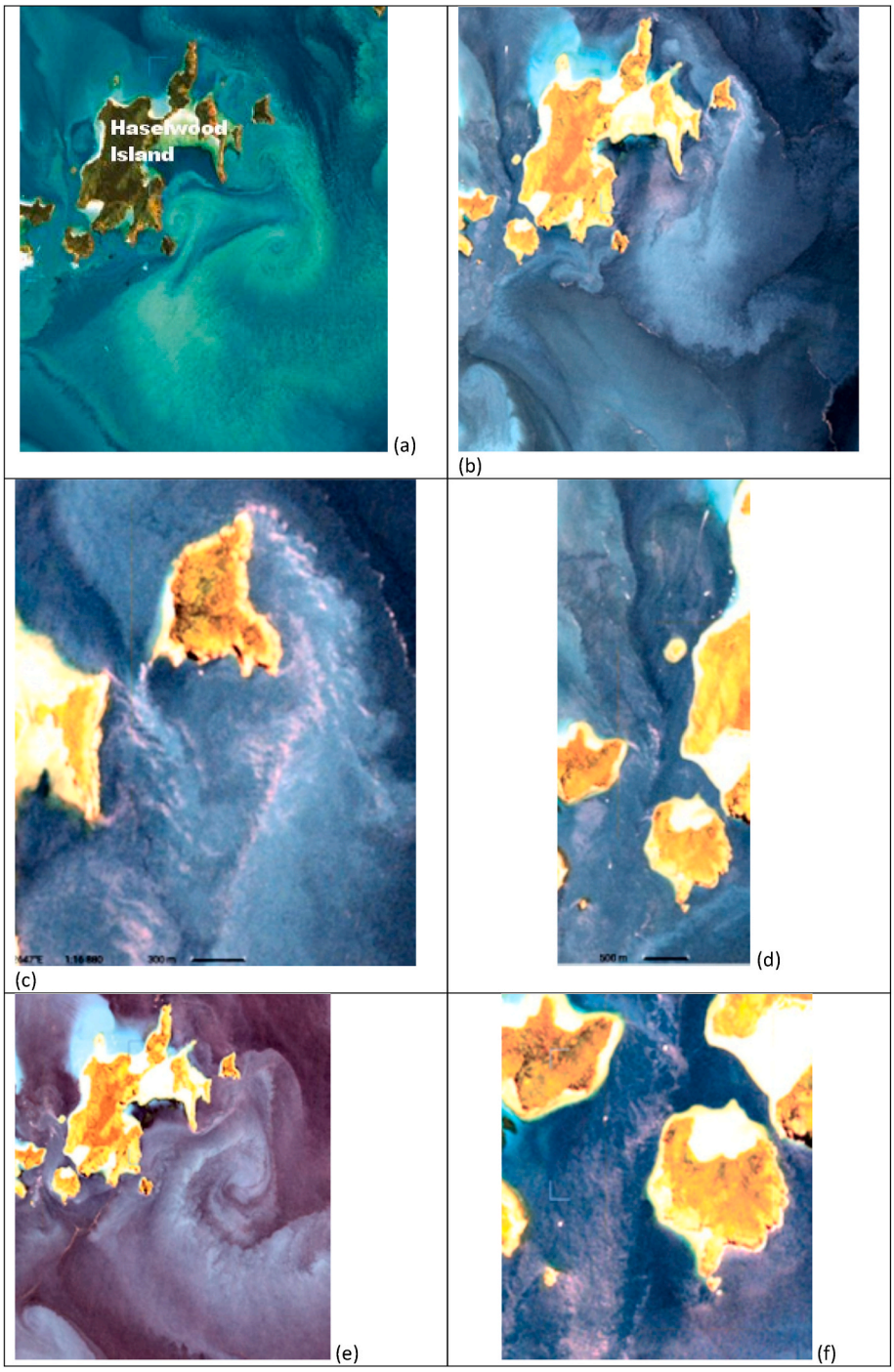

Fig. 4. Sentinel-2 satellite images of turbidity plumes around Haselwood Island showing (a-b) mushroom tidal jets reversing direction with the tides to the south of the island, (c) separating flows past headlands and a developing jet in the reef passage between Lupton Island a Workington Reef, (d) the tidal jet between the west coast of Haselwood island and Whitsunday Island to the east at ebb tide, which generates an eddy on the west coast of Haselwood Island, (e) the large eddy to the south of the island near slack tide, (f) the tidal jet between Haselwood Island and Whitsunday Island to the west at flood tide that bypasses Teague Island.

observed flow patterns shown in Fig. 5 were well reproduced by the model. The four particle seeding points were located in the bays (Fig. S2a) because everywhere else there is swift flushing. The file Animation S4 shows the predicted particle plume over 240 h during calm weather, at 1 h interval for the first 12 h (1 spring tidal cycle), and at 12 h interval afterwards. The model predicted that bays 1 and 3 retained about 7% of the virtual larvae after 8 days, hence these bays were self-seeded; bay 2 was nearly flushed out after 8 days, hence it was marginally self-seeded; and bay 4 was flushed out after 1 tidal cycle, thus it was not self-seeded.

iii Magnetic Island

Magnetic Island (Fig. S3) has several bays, the largest bays being Geoffrey Bay and Horseshoe Bay. The bathymetry and the model mesh around Magnetic Island are shown in Fig. S4. These two bays are encompassed between rocky headlands that are 3.13 km apart in Horseshoe Bay and 3.71 km apart in Geoffrey Bay. Satellite images (Fig. 5) revealed that the reversing tidal currents generated mushroom jets and eddies at the headlands and free shear layers in coastal waters, and these transient features occasionally penetrated the bays.

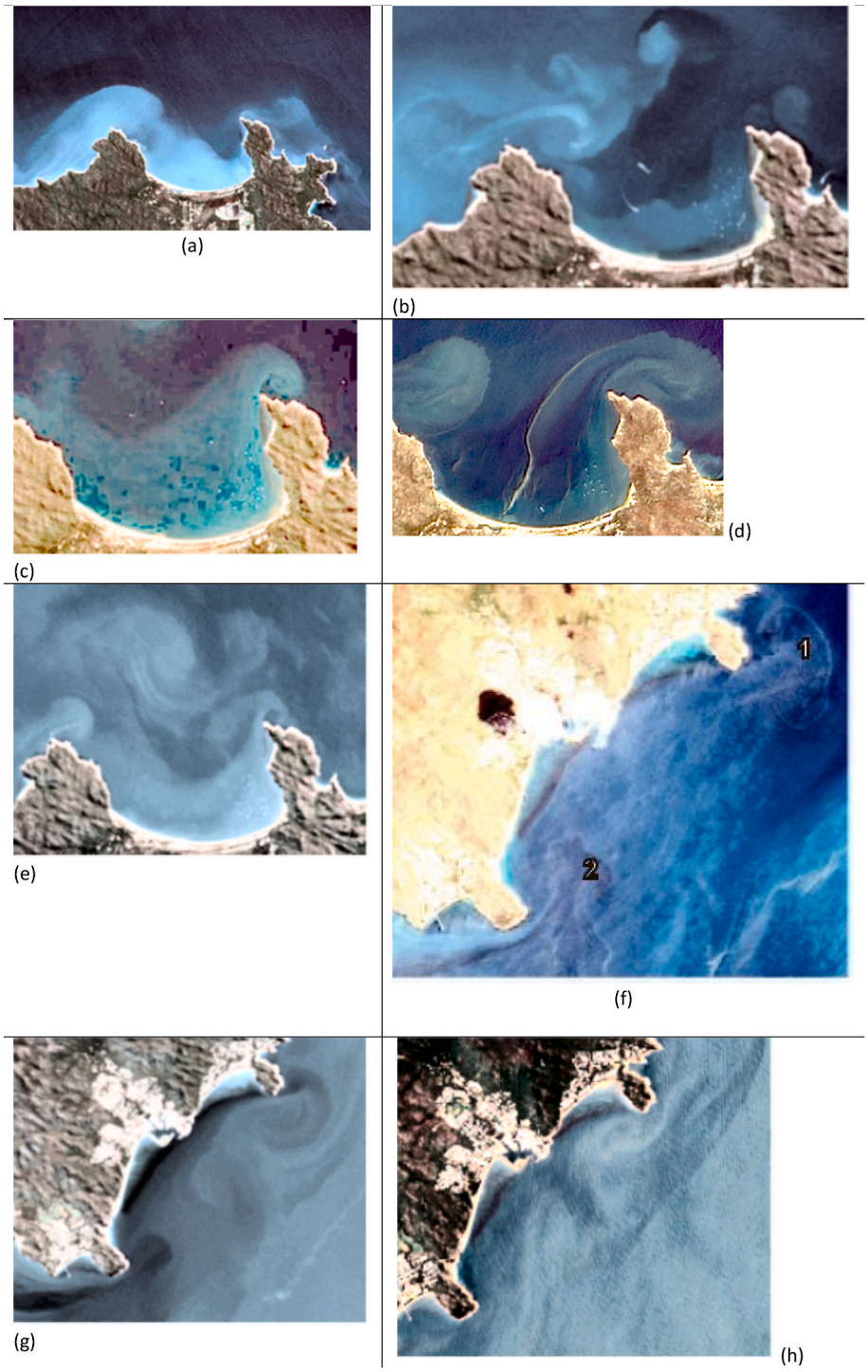

Fig. 5. With North up the page, typical Sentinel-2 images of Horseshoe Bay showing (a-b) coastal water entering the bay from the west at ebb tide, (c-d) a tidal jet of width half that of the bay flushing water out of the bay on the ebb tide and water entering the bay from the west, (e) 'fossil' turbulence offshore at slack high tide. Sentinel-2 images of Geoffrey Bay showing, (f) at ebb tide, a mushroom jet entering the bay past the headland to the south and another mushroom jet exiting the bay past the headland to the north, and, at flood tide, the incoming tidal water bypasses the headland to the north and enters the bay as a jet of clear nearshore waters (g) in its top half and (h) in the middle of the bay. In (f), the letters 1 and 2 point to the outgoing and incoming, respectively, mushroom jets downstream of headlands.

The SLIM model of Schlaefer et al. (2021) was used with a more refined mesh in Horseshoe Bay. The predicted currents in and around Horseshoe Bay during one tidal cycle for an average tide and in calm weather are shown in the file Animation S5. The jet shed by the headland to the west at flood tide penetrated Horseshoe Bay and it swiftly flushes out the bay at ebb tide. Virtual passive larvae were released at one site in Horseshoe Bay and two sites in Geoffrey Bay (Fig. S3). The file Animation S6 shows the evolution of the predicted larval plumes at 1 h interval over 48 h. It is apparent that Horseshoe Bay was flushed very swiftly, within one tidal cycle; thus, that bay was not self-seeded. In contrast, Geoffrey Bay was flushed much slower with some particles flushed out at ebb tide returning into the bay at flood tide. The number of such particles diminished progressively in successive tidal cycles, but it did not vanish (Fig. 6). After 8 days, 0.23 % of the particles still

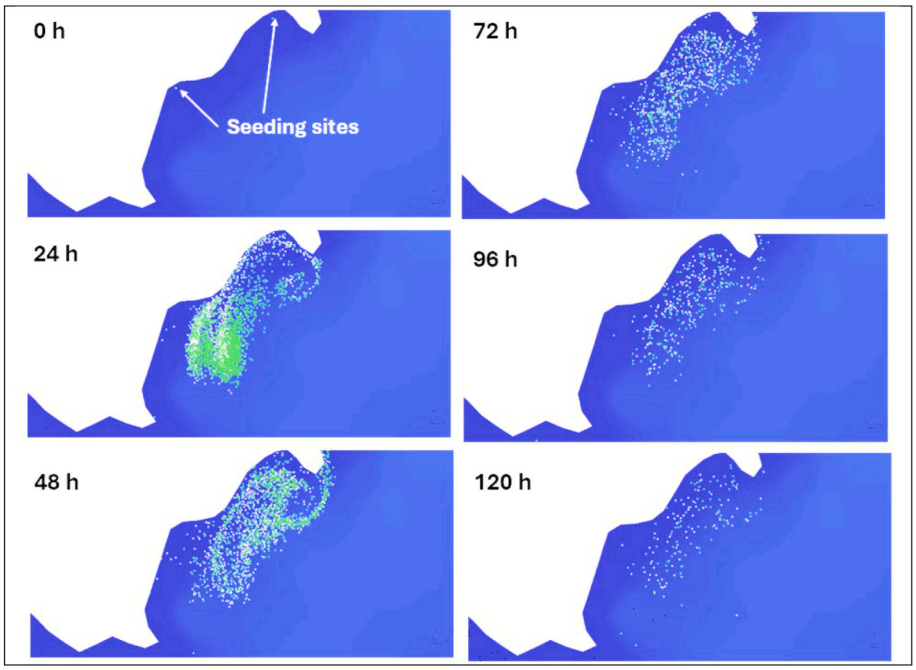

Fig. 6. Plots at 24 h interval of the location of the virtual larvae at high tide in Geoffrey Bay in calm weather after seeding at the sites shown in Fig. S3.

remained in the bay. Thus, Geoffrey Bay was slightly self-seeded during calm weather.

iv Ribbon Reef No. 10

Having examined above the key role of embayments to enable self-recruitment, here we study whether passive larvae from a long and relatively straight reef, longer than the tidal excursion, can self-recruit. The best candidate for that is Ribbon No. 10 Reef, which is the longest (29.3 km) ribbon reef in the whole GBR. It is thus much longer than the typical tidal excursion length of 5–7 km. It is located at the shelf edge of the northern GBR, southeast of Lizard Island (Fig. 7a). Its long axis is oriented in the north-south direction, perpendicular to the tidal currents. In calm weather, the currents around Ribbon No. 10 Reef were mostly driven by the tides and intruding ocean water that generated a prevailing southward longshore current (Fig. 7a; Wolanski and Pickard, 1985). In the northern passage at flood tide, a tidal jet occurred that was deflected southward by the prevailing longshore current (Fig. 7b). Near the end of the flood tide the jet formed a boundary layer along the western edge of the reef and at ebbing tide the northern passage drained away that boundary layer (Fig. 7c). The tidal inflow in the southern passage mostly bypassed the first channel and flows landward through the second and third passages (Fig. 7d). In contrast, at ebb tide, the flow in the southern passage came from all channels to form one large jet seaward of the reef (Fig. 7e). These flow patterns were also well reproduced by the SLIM model with a mesh size of 150 m near reefs, as shown in the file Animation S7. The model was further verified using the current meter data of Wolanski and Pickard (1985) near Lizard Island (not shown).

The virtual passive larvae were released at three locations along the length of the reef, namely to the north, in the middle, and to the south of the reef. The file Animation S8 shows the evolution of the larval plumes at 30-min intervals for a period of two weeks. It is apparent that waterborne particles close to the northern and southern passages were swiftly flushed away; thus, the northern and southern sides of the reef were not self-seeded. In contrast, the virtual larvae particles spawned in the middle of the reef were trapped for up to 9 days, and this included 4 days traversing a small lagoon in the reef. Thus, the middle region of the reef was self-seeded, but only because of the presence of a small embayment in the reef (the small lagoon).

v Tijou Reef, Cockatoo Reef and Bligh Reef

Clear evidence for the retention of passive particles at small spatial scales was found at Tijou Reef. Tijou Reef is a 22 km long ribbon reef at the shelf edge of the far northern GBR with marked indentations along its length (Fig. 1c and S7). For model verification, we used the current meter data of Wolanski and Lambrechts (2020). These data revealed that the circulation was driven by the tides, the wind, the oceanic swell waves breaking over the outer reef crest, and the circulation in the Coral Sea (Wolanski et al., 2024). There were periods, lasting typically 1–2 weeks especially in October–November, which included the mass coral spawning season, of calm weather when the net currents in the Coral Sea next to the Tijou Reef were negligible (Wolanski et al., 2024). Such a period is evidenced in the satellite image (Fig. 8) that shows reef-perpendicular streak lines over the reef flat, which indicates a seaward tidal flow over the reef flat, and reef-parallel streak lines aggregating the material brought in from the reef flat, an indication of weak currents seaward from the reef at the time of this satellite image (Wolanski and Hamner, 1988). Fig. 8 also shows mushroom tidal jets in the reef passages to the south.

The file Animation S9 shows the predicted currents around and over Tijou Reef at 1 h interval over a tidal cycle as predicted by the SLIM model of Wolanski et al. (2017); the colour bar shows the speed in m/s. The file Animation S10 shows over 168 h at 1 h interval for the first 12 h, and at 12 h intervals afterwards, the predicted larval plume after a one-off spawning at two sites (the two embayments of Tijou Reef on the landward site). Clearly, the concave-shaped oval bowls retained some particles in calm weather and no other location did so.

A similar case to Tijou Reef is Cockatoo Reef in the southern GBR. Satellite images revealed that it has a concave bowl curving landward and sharp headlands; it trapped water and its larvae inside the bowl where weak currents apparently prevailed, while strong currents may occur elsewhere (Fig. 8c). This trapping occurred in the bowl of the reef because the reef passage is perpendicular to the reef axis. If the reef passage is not perpendicular to the reef axis, as is the case of Bligh Reef in the far northern GBR (Fig. 8d), the tidal jet flows straight into the bowl parallel to the reef, and the bowl is thus swiftly flushed.

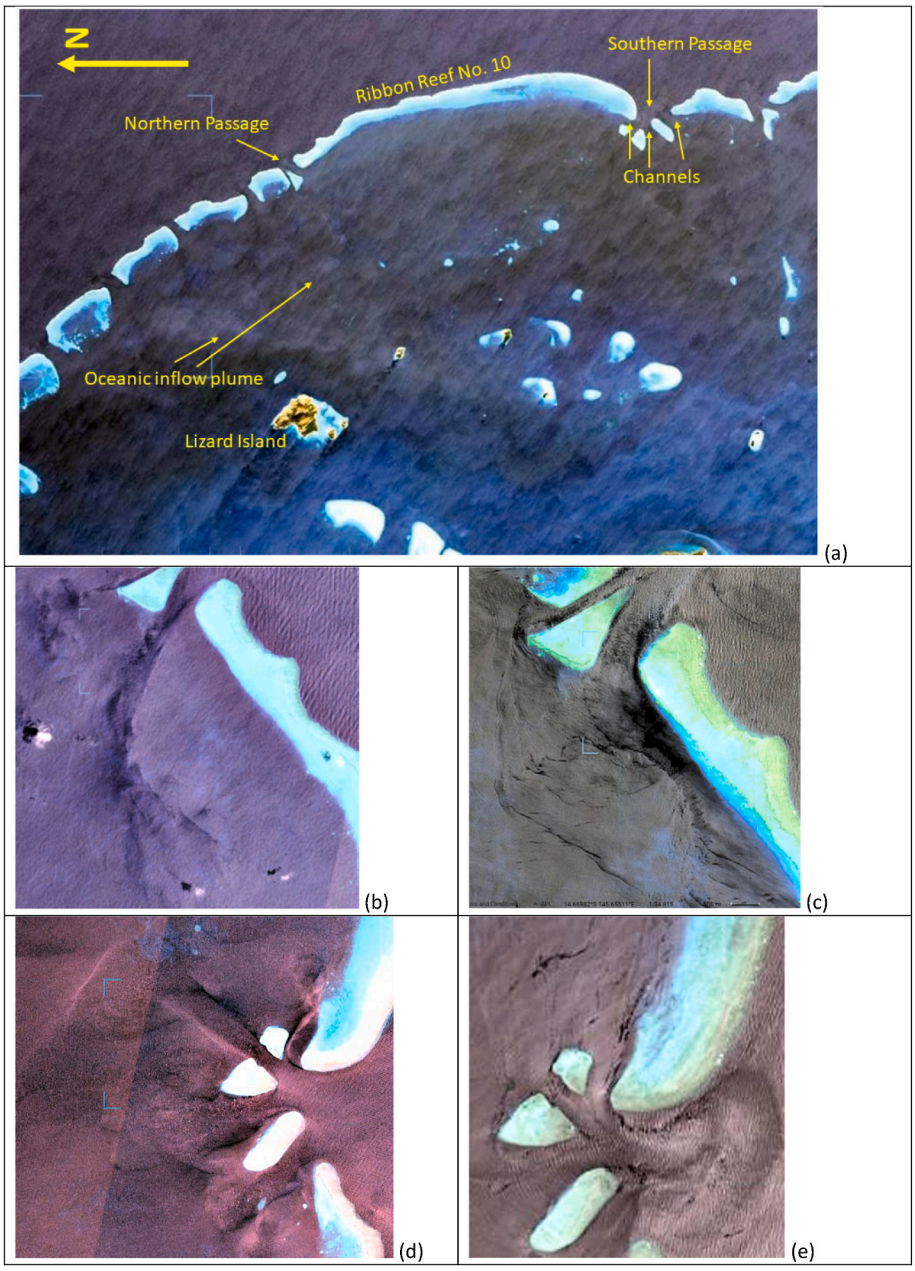

Fig. 7. (a) Landsat image of the area around Ribbon Reef No. 10 and Lizard Island showing the prevailing oceanic inflow in calm weather. Sentinel-2 images of (b) the flood tidal jet through the northern passage that is deflected longshore southward, (c) the reef boundary layer water drawn out by the ebb tidal jet through the northern passage, (d) the flood tidal jets through the channels of the southern passage but largely bypassing the first channel, (e) the ebb tidal jets through channels of the southern passage that aggregate to form one large jet seaward, all images in calm weather.

4. Discussion

This study on the potential for self-recruitment of passive larvae at small spatial scales (100s of m) relied on satellite and oceanographic modeling data at a number of sites in the GBR. The study provided results that enabled one to quantify which reef or island in the GBR may be self-seeding for passive (i.e., not swimming) water-borne larvae such as those of broadcast coral and crown-of-thorns starfish. It is known that these larvae generally cannot remain behind an island or reef for the pelagic larval duration. This is because tidal eddies behind an island or reef do not trap water-borne larvae for more than 6 h (half a tidal cycle) as the eddies do not flip from one site of the island or reef to the other when the tide reverses; instead, they are swiftly advected away from the island or reef, possibly because they have the opposite rotation sign on either side of the island (Hamner and Hauri, 1981; Wolanski et al., 2024). Thus, reefs or islands with no embayments are not self-seeding at small spatial scales. Indeed, the 29 km long Ribbon Reef No. 10, which is the longest and nearly straight reef in the GBR, is self-seeding only near the middle of the reef and then only because of a lagoon in that area.

Embayments (bays) and/or headlands are needed to trap water and its larvae near reefs. Even with an embayment or headland, self-recruitment may not occur. The location of the embayment, its size and shape, and those of the headlands defining the embayments, and the magnitude and direction of the surrounding currents, all have to be 'just right' for the local hydrodynamics to generate self-recruitment. In Orpheus Island, only one bay (Pioneer Bay, and then only its northern half), is self-seeding. There are swift tidal currents parallel to the mouth of the bay. The key factor that differentiates that bay from the other bays is that its aspect ratio = Length/Width ≈1 (Fig. 9a), while all the other bays have an aspect ratio ≪ 1. When the tidal currents are fully

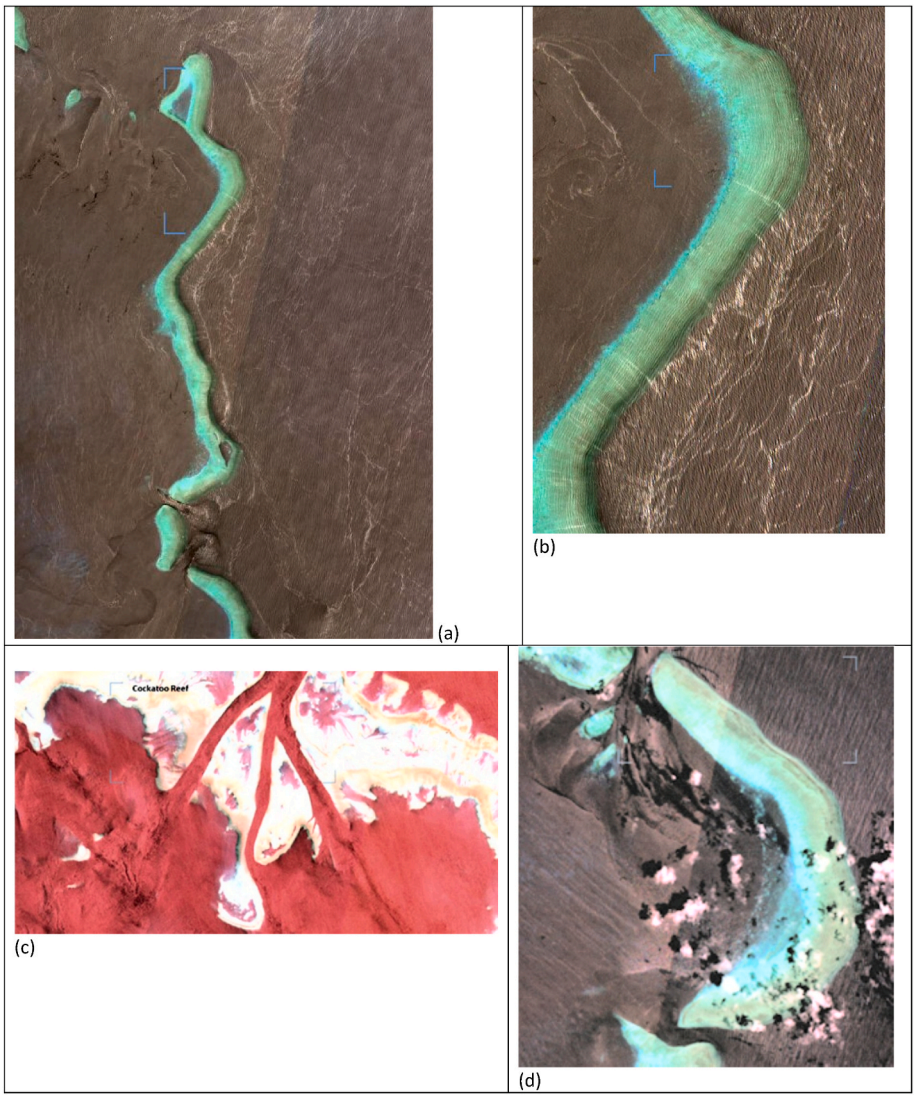

Fig. 8. (a) A Sentinel-2 image of Tijou Reef at ebb tide. (b) A zoom-in view of (a) reveals the streamlines over the reef flat. (c) Sentinel-2 image of Cockatoo Reef showing tidal jets through reef passages and eddies trapping water at flood tide in the bowl of concave reefs. The embayment of Cockatoo Reef is 5 km wide from tip to tip. (d) Sentinel-2 image of Bligh Reef showing the tidal jet at flood tide at the northern reef passage intruding in the bowl of the concave reef and thus likely swiftly flushing it. The embayment is 6.7 km wide from tip to tip. North is up the page.

established, a separation streamline occurs at the mouth of the bay that inhibits mixing between bay water and coastal water. This generates a weak eddy in the bay. At that stage, the situation resembles that of the steady currents behind a groyne in a river with a steady flow (Fig. 9b; Uijttewaal, 2005). A sharp separation streamline occurs and mixing between the water behind the groyne and the water in the river is slow and controlled by the meandering of the separation streamline. When the flow is tidal, this trapping behind a headland is decreased by the creation of a mushroom tidal jet that forms when the tidal currents accelerate past the headland. The jet has an eddy on the island side that can penetrate the bay and swiftly flush it out (Fig. 9c). This flushing by the mushroom jet is the reason that the southern side of Pioneer Bay is not self-seeding.

Further, the study at Haselwood Island reveals that the relative orientation of the bay compared to that of the tidal currents outside the bay is also important. When the bay axis is not perpendicular to the tidal currents, the tidal currents penetrated the bay up to a point where the pressure gradient switched from favouring to adverse; at that point the intruding flow separated from the coast (Fig. 9d; Signell and Geyer, 1991; Davies et al., 1995; Coutis and Middleton, 2002; Stansby et al., 2016). This is also the reason why Horseshoe Bay is swiftly flushed, though that bay has an aspect ratio ≈1; indeed, the entrance to the bay on the west side is oblique (and not perpendicular) to the tidal currents, thus allowing for the ebb tidal currents to directly penetrate the bay. The degree of elf-seeding at small spatial scales thus depends on many parameters, including the details of the incident flow, the shape of the headlands, the relative orientation of the reef compared to that of the tidal currents in proximity, the aspect ratio, and the time that the mushroom tidal jet is in front of the embayment. Finally, the flushing of an embayment can take several tidal cycles. When the net coastal currents are small, some bay water that was flushed out of the bay at ebb tide returns to the bay at the following flood tide. Over successive tidal cycles, the amount of bay water that returns becomes smaller. The resulting flushing rate can be quantified using methods developed by estuarine oceanographers using two parameters, namely the residence time, i.e., the time it takes for 37% of the particles to leave the estuary for the first time (some particles later return with the reversing tides), and the exposure time, i.e. the time spent in the estuary until the particles never return back in the embayment (de Brauwere et al., 2011; Wolanski and Elliott, 2015).

Thus, the details of the fluid dynamics at small scales (typically 150–200 m) determine whether a reef, or part of a reef, is – or is not –

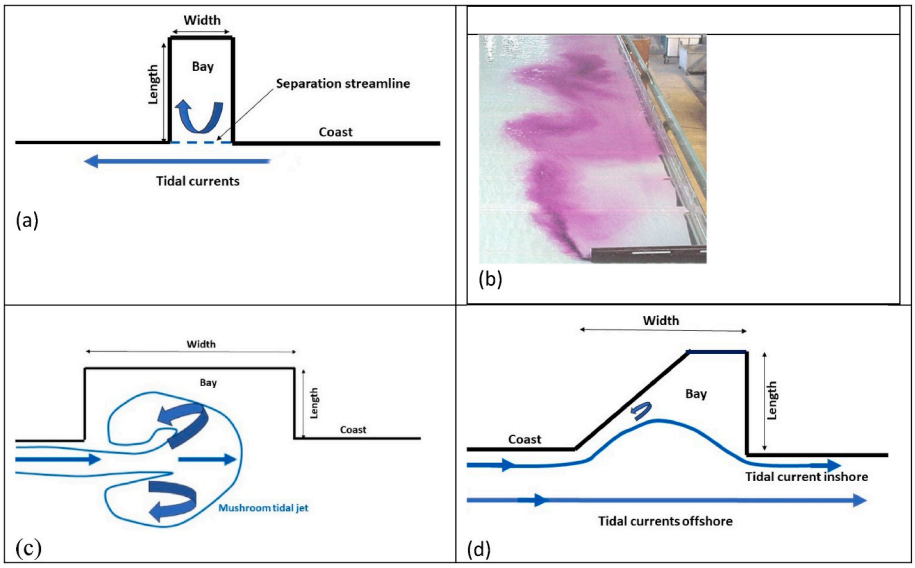

Fig. 9. (a) When the tidal currents are fully established and flow parallel to the mouth of the bay, a sharp separation streamline separates the water inside and outside of the bay and an eddy is generated in the bay. (b) In steady flows in a river protected by groynes, a sharp front separates the river water from the sheltered water, and mixing is due to the meandering of the front. (Photo courtesy of Wim S.J. Uijttewaal). (c) For self-recruitment, a bay needs to be long enough to prevent flushing by the landward eddy in the tidal mushroom jet that develops when the coastal current accelerates after slack tide. (d) A bay oblique to the tidal currents inhibits flow separation, and this enables the intrusion of the tidal currents, which results in the swift flushing of the bay.

self-seeded. Studies of the degree of self-recruitment in the GBR need to focus on the fine-scale hydrodynamics. However, GBR oceanographic research has focused so far mainly on much larger spatial scales while focusing on the connectivity between reefs. Hence, we have a vast knowledge gap about reef self-recruitment in the GBR.

The small spatial scales control the degree of self-recruitment in a reef or island. Research on the GBR biophysics has much to learn from the vast knowledge of small-scale hydrodynamics in estuarine oceanography and river engineering. This study suggests that the self-recruitment of passive, water-born larvae is not a common occurrence in the GBR. When self-recruitment occurs, it is very localized, depending on the details of the local bathymetry and oceanography. Therefore, for self-recruitment, every reef or island is an individual case; there are no simple single-parameter rules. From a management perspective, some reefs have multiple zones of protection and our findings of self-recruitment at small spatial scales may be relevant to select sites for coral restoration where the conditions favour self-recruitment (Harrison, 2024; Quigley and Donelson, 2014). The final selection of these sites and species could be additionally refined by selecting those sites likely to be least impacted by the pollutants and the physical and chemical stressors that they will face in the future (Byrne et al., 2024; Hoogenboom et al., 2024; Kamenos and Hennige, 2024).

Our investigation has focused in on passive particles and the likelihood of self-recruitment at local scales, which was generally low. In contrast, non-passive particles, such as reef fish larvae at post-flexion, swim directionally using auditory and chemical cues towards their natal reefs (Kingsford et al., 2024). Thus, their self-recruitment is typically orders of magnitude larger than that for passive larvae (Wolanski and Kingsford, 2014).

In our study, a lack of self-recruitment at small spatial scales by passive particles did not negate higher levels of connectivity at the scales of reefs (kilometres) and clusters of reefs (10s to of kilometres). These larger spatial scales may be more relevant to managers of reef resources for the determination of source reefs and the like. For reefs located in close proximity to each other, so as to form an archipelago, the 'sticky water effect' will promote the retention of the passive larvae in the archipelago (Andutta et al., 2012). However, the larvae may not actually recruit to their natal reefs but instead recruit throughout the archipelago; in that case self-recruitment is for the whole archipelago and not for an individual reef.

CRediT authorship contribution statement

Eric Wolanski: Writing – review & editing, Writing – original draft, Visualization, Validation, Formal analysis, Conceptualization. **Miguel De Le Court:** Visualization, Investigation. **Jonathan Lambrechts:** Validation, Investigation, Conceptualization. **Michael Kingfsord:** Writing – review & editing, Investigation, Conceptualization.

Declaration of competing interest

The authors declare that they have no known competing financial interests or personal relationships that could have appeared to influence the work reported in this paper.

Data availability

Data will be made available on request.

Appendix A. Supplementary data

Supplementary data to this article can be found online at https://doi.org/10.1016/j.ecss.2024.108976.

References

Andutta, F., Ridd, P.V., Wolanski, E., 2011. Dynamics of hypersaline coastal waters in the Great Barrier Reef. Estuarine. Coast. Shelf Sci. 94, 299–305.
Andutta, F., Kingsford, M., Wolanski, E., 2012. 'Sticky water' enables the retention of larvae in a reef mosaic. Estuarine. Coast. Shelf Sci. 101, 54–63.
Ani, C.J., Haller-Bull, V., Gilmour, J.P., Robson, B.J., 2024. Connectivity modelling identifies sources and sinks of coral recruitment within reef clusters. Sci. Rep. 14, 13564.
Bode, M., Leis, J.M., Mason, L.B., Williamson, D.H., Harrison, H.B., Choukroun, S., Jones, G.P., 2019. Successful validation of a larval dispersal model using genetic parentage data. PLoS Biol. 17 (7), e3000380.
Bottesch, M., Gerlach, G., Halbach, M., Bally, A., Kingsford, M.J., Mouritsen, H., 2016. A magnetic compass that might help coral reef fish larvae return to their natal reef. Curr. Biol. 26 (24), R1266–R1267.
Burgess, S.C., Kingsford, M.J., Black, K.P., 2007. Influence of tidal eddies and wind on the distribution of presettlement fishes around One Tree Island, Great Barrier Reef. Mar. Ecol. Prog. Ser. 341, 233–242.

Byrne, M., Foo, S.A., Vila-Concejo, A., Wolfe, K., 2024. Impacts of climate change stressors on the Great Barrier reef. In: Wolanski, E., Kingsford, M. (Eds.), Oceanographic Processes of Coral Reefs. Physical and Biological Links in the Great Barrier Reef. CRC Press, Boca Raton, London & New York, pp. 323–340.
Coutis, P.F., Middleton, J.H., 2002. The physical and biological impact of a small island wake in the deep ocean. Deep Sea Res. Oceanogr. Res. Pap. 49 (8), 1341–1361.
Davies, P.A., Dakin, J.M., Falconer, R.A., 1995. Eddy formation behind a coastal headland. J. Coast Res. 11 (1), 154–167.
de Brauwere, A., de Brye, B., Blaise, S., Deleersnijder, E., 2011. Residence time, exposure time and connectivity in the Scheldt Estuary. J. Mar. Syst. 84 (3–4), 85–95.
Galloway, D., Wolanski, E., King, B., 1996. Modelling eddy formation in coastal waters: a comparison between model capabilities. In: Spaulding, M., Cheng, R.T. (Eds.), Estuarine and Coastal Modelling. American Society Civil Engineers, pp. 13–25.
Green, A.L., Maypa, A.P., Almany, G.R., Rhodes, K.L., Weeks, R., Abesamis, R.A., Gleason, M.G., Mumby, P.J., White, A.T., 2015. Larval dispersal and movement patterns of coral reef fishes, and implications for marine reserve network design. Biol. Rev. 90 (4), 1215–1247.
Gerlach, G., Atema, J., Kingsford, M.J., Black, K.P., Miller-Sims, V., 2007. Smelling home can prevent dispersal of reef fish larvae. Proc. Natl. Acad. Sci. USA 104 (3), 858–863.
Hamner, W.M., Hauri, I.R., 1977. Fine-scale surface currents in the Whitsunday Islands, Queensland, Australia: effect of tide and topography. Aust. J. Mar. Freshw. Res. 28 (3), 333–359.
Hamner, W.M., Hauri, I.R., 1981. Effects of island mass: water flow and plankton pattern around a reef in the Great Barrier Reef lagoon, Australia. Limnol. Oceanogr. 26, 1084–1102.
Harrison, P.L., 2024. Sexual reproduction of reef corals and application to coral restoration. In: Wolanski, E., Kingsford, M. (Eds.), Oceanographic Processes of Coral Reefs. Physical and Biological Links in the Great Barrier Reef`. CRC Press, Boca Raton, London & New York, pp. 419–437.
Hoogenboom, M.O., Osipova, L., Nordborg, M., Schlaefer, J.A., Critchell, K., 2024. Dispersal and environmental impacts of pan-oceanic contaminants. In: Wolanski, E., Kingsford, M. (Eds.), Oceanographic Processes of Coral Reefs. Physical and Biological Links in the Great Barrier Reef`. CRC Press, Boca Raton, London & New York, pp. 143–150.
Jones, G.P., Planes, S., Thorrold, S.R., 2005. Coral Reef fish larvae settle close to home. Curr. Biol. 15 (14), 1314–1318.
Kamenos, N.A., Hennige, S.J., 2024. A historical perspective on thermal and heatwave-induced bleaching on the Great Barrier Reef. In: Wolanski, E., Kingsford, M. (Eds.), Oceanographic Processes of Coral Reefs. Physical and Biological Links in the Great Barrier Reef`. CRC Press, Boca Raton, London & New York, pp. 282–289.
Karkarey, R., Theo, A.H., 2016. Homeward bound: fish larvae use dispersal corridors when settling on coral reefs. Front. Ecol. Environ. 14 (10), 569–570.
Kingsford, M.J., Spiecker, L., Gerlach, G.G., 2024. In: Wolanski, E., Kingsford, M.J. (Eds.), Oceanographic Processes of Coral Reefs. Physical and Biological Links in the Great Barrier Reef. CRC Press, Boca Raton, London & New York, pp. 260–271.
Lambrechts, J., Hanert, E., Deleersnijder, E., Bernard, P.-E., Legat, V., Remacle, J.-F., Wolanski, E., 2008. A multi-scale model of the hydrodynamics of the whole Great Barrier Reef. Estuarine. Coast. Shelf Sci. 79, 143–151.
Leis, J.M., Siebeck, U., Dixson, D.L., 2011. How Nemo finds home: the neuroecology of dispersal and of population connectivity in larvae of marine fishes. Integr. Comp. Biol. 51 (5), 826–843.
McGowan, A., Lanyon, J., Clark, N., Blair, D., Marsh, H., Wolanski, E., Seddon, J., 2023. Seascape genetics of a mobile marine mammal: evidence of barriers to dugong gene flow along the Queensland coast. Marine Mammal Science 39 (3), 918–939.
Nozawa, Y., Okubo, N., 2011. Survival dynamics of reef coral larvae with special consideration of larval size and the genus *Acropora*. Biol. Bull. 220 (1), 15–22.
Okubo, A., 1971. Oceanic diffusion diagrams. Deep Sea Res. Oceanogr. Abstr. 18 (8), 789–802.
Paris, C.B., Chérubin, L.M., Cowen, R.K., 2007. Surfing, spinning, or diving from reef to reef: effects on population connectivity. Mar. Ecol. Prog. Ser. 347, 285–300.
Pratchett, M.S., Chandler, J.F., Choukroun, S.M., Doll, P.C., et al., 2024. Biophysical processes involved in the initiation and spread of population irruptions of crown-of-thorns starfish on the Great Barrier Reef. In: Wolanski, E., Kingsford, M. (Eds.), Oceanographic Processes of Coral Reefs. Physical and Biological Links in the Great Barrier Reef`. CRC Press, Boca Raton, London & New York, pp. 290–305.
Quigley, K.M., Donelson, J.M., 2014. Selective breeding and promotion of naturally heat-tolerant coral reef species. In: Wolanski, E., Kingsford, M. (Eds.), Oceanographic Processes of Coral Reefs. Physical and Biological Links in the Great Barrier Reef`. CRC Press, Boca Raton, London & New York, pp. 341–357.
Reichelt, R.W., Bradbury, R.H., Moran, P.J., 1990. The crown-of-thorns starfish, *Acanthaster planci*, on the Great Barrier reef. Math. Comput. Model. 13 (6), 45–60.
Saint-Amand, A., Lambrechts, J., Hanert, E., 2023. Biophysical models resolution affects coral connectivity estimates. Sci. Rep. 13 (1), 9414.
Schlaefer, J.A., Wolanski, E., Lambrechts, J., Kingsford, M.J., 2018. Wind conditions on the Great Barrier Reef influenced the recruitment of snapper (*Lutjanus carponotatus*). Front. Mar. Sci. 5, 193.
Schlaefer, J.A., Wolanski, E., Lambrechts, J., Kingsford, M.J., 2021. Behavioural and oceanographic isolation of an island-based jellyfish (*Copula sivickisi*, Class Cubozoa) population. Sci. Rep. 11, 10280.
Signell, R.P., Geyer, W.R., 1991. Transient eddy formation around headlands. J. Geophys. Res. Oceans 96 (C2), 2561–2575.
Spiecker, L., Curdt, F., Bally, A., Janzen, N., Kraemer, P., Leberecht, B., Kingsford, M.J., Mouritsen, H., Winklhofer, M., Gerlach, G., 2023. Coral reef fish larvae show no evidence for map-based navigation after physical displacement. iScience 26, 106950.
Stansby, P., Chini, N., Lloyd, P., 2016. Oscillatory flows around a headland by 3D modelling with hydrostatic pressure and implicit bed shear stress comparing with experiment and depth-averaged modelling. Coast. Eng. 116, 1–14.
Uijttewaal, W.S., 2005. Effects of groyne layout on the flow in groyne fields: laboratory experiments. J. Hydrau. Eng. -ASCE. 131 (9), 782.
White, L., Wolanski, E., 2008. Flow separation and vertical motions in a tidal flow interacting with a shallow-water island. Estuar. Coast Shelf Sci. 77, 457–466.
Wolanski, E., Pickard, G.L., 1985. Long-term observations of currents on the central Great Barrier Reef continental shelf. Coral Reefs 4, 47–57.
Wolanski, E., Hamner, W., 1988. Topographically controlled fronts and their biological influence. Science 241, 177–181.
Wolanski, E., Spagnol, S., 2000. Sticky waters in the Great Barrier Reef. Estuarine. Coast. Shelf Sci. 50, 27–32.
Wolanski, E., Kingsford, M.J., 2014. Oceanographic and behavioural assumptions in models of the fate of coral and coral reef fish larvae. J. R. Soc. Interface 11, 20140209.
Wolanski, E., Imberger, J., Heron, M., 1984. Island wakes in shallow coastal waters. J. Geophys. Res. 89 (C6), 10553–10569.
Wolanski, E., Asaeda, T., Tanaka, T., Deleersnijder, E., 1996. Three-dimensional island wakes in the field, laboratory and numerical models. Continent. Shelf Res. 16, 1437–1452.
Wolanski, E., Lambrechts, J., Thomas, C., Deleersnijder, E., 2013. The net water circulation through Torres Strait. Continent. Shelf Res. 64, 66–74.
Wolanski, E., Elliott, M., 2015. Estuarine Ecohydrology. An Introduction. Elsevier, Amsterdam, p. 322.
Wolanski, E., Andutta, F., Deleersnijder, E., Li, Y., Thomas, C.J., 2017. The gulf of Carpentaria heated torres strait and the northern Great Barrier Reef during the 2016 mass coral bleaching. Estuar. Coast Shelf Sci. 194, 172–181.
Wolanski, E., Lambrechts, J., 2020. The net water circulation in the far northern Great Barrier Reef. Estuarine. Coast. Shelf Sci. 235, 106569.
Wolanski, E., Kingsford, M., Lambrechts, J., Marmorino, G., 2024. The physical oceanography of the Great Barrier Reef: a review. In: Wolanski, E., Kingsford, M. (Eds.), Oceanographic Processes of Coral Reefs. Physical and Biological Links in the Great Barrier Reef`. CRC Press, Boca Raton, London & New York, pp. 9–34.